Synthesis and properties of $La_{1-x}Sr_xNiO_3$ and $La_{1-x}Sr_xNiO_2$

Mengwu Huo(霍梦五), Zengjia Liu(刘增家), Hualei Sun(孙华蕾), Lisi Li(李历斯), Hui Lui(刘晖), Chaoxin Huang(黄潮欣), Feixiang Liang(梁飞翔), Bing Shen(沈冰), and Meng Wang(王猛)

Citation: Chin. Phys. B, 2022, 31 (**10**): 107401. DOI: 10.1088/1674-1056/ac7a1a
Journal homepage: http://cpb.iphy.ac.cn; http://iopscience.iop.org/cpb

What follows is a list of articles you may be interested in

Superconductivity and unconventional density waves in vanadium-based kagome materials AV_3Sb_5

Hui Chen(陈辉), Bin Hu(胡彬), Yuhan Ye(耶郁晗), Haitao Yang(杨海涛), and Hong-Jun Gao(高鸿钧)
Chin. Phys. B, 2022, 31 (**9**): 097405. DOI: 10.1088/1674-1056/ac7f95

Josephson vortices and intrinsic Josephson junctions in the layered iron-based superconductor $Ca_{10}(Pt_3As_8)((Fe_{0.9}Pt_{0.1})_2As_2)_5$

Qiang-Tao Sui(随强涛) and Xiang-Gang Qui(邱祥冈)
Chin. Phys. B, 2022, 31 (**9**): 097403. DOI: 10.1088/1674-1056/ac76ae

Conservation of the particle-hole symmetry in the pseudogap state in optimally-doped $Bi_2Sr_2CuO_{6+\delta}$ superconductor

Hongtao Yan(闫宏涛), Qiang Gao(高强), Chunyao Song(宋春尧), Chaohui Yin(殷超辉), Yiwen Chen(陈逸雯), Fengfeng Zhang(张丰丰), Feng Yang(杨峰), Shenjin Zhang(张申金), Qinjun Peng(彭钦军), Guodong Liu(刘国东), Lin Zhao(赵林), Zuyan Xu(许祖彦), and X. J. Zhou(周兴江)
Chin. Phys. B, 2022, 31 (**8**): 087401. DOI: 10.1088/1674-1056/ac7214

Photothermal-chemical synthesis of P-S-H ternary hydride at high pressures

Tingting Ye(叶婷婷), Hong Zeng(曾鸿), Peng Cheng(程鹏), Deyuan Yao(姚德元), Xiaomei Pan(潘孝美), Xiao Zhang(张晓), and Junfeng Ding(丁俊峰)
Chin. Phys. B, 2022, 31 (**6**): 067402. DOI: 10.1088/1674-1056/ac5604

Experimental observation of pseudogap in a modulation-doped Mott insulator: Sn/Si(111)-($\sqrt{30}\times\sqrt{30}$)*R*30°

Yan-Ling Xiong(熊艳翎), Jia-Qi Guan(关佳其), Rui-Feng Wang(汪瑞峰), Can-Li Song(宋灿立), Xu-Cun Ma(马旭村), and Qi-Kun Xue(薛其坤)
Chin. Phys. B, 2022, 31 (**6**): 067401. DOI: 10.1088/1674-1056/ac65f2

Synthesis and properties of $La_{1-x}Sr_xNiO_3$ and $La_{1-x}Sr_xNiO_2$

Mengwu Huo(霍梦五), Zengjia Liu(刘增家), Hualei Sun(孙华蕾), Lisi Li(李历斯), Hui Lui(刘晖), Chaoxin Huang(黄潮欣), Feixiang Liang(梁飞翔), Bing Shen(沈冰), and Meng Wang(王猛)†

Center for Neutron Science and Technology, Guangdong Provincial Key Laboratory of Magnetoelectric Physics and Devices, School of Physics, Sun Yat-Sen University, Guangzhou 510275, *China*

(Received 29 April 2022; revised manuscript received 8 June 2022; accepted manuscript online 18 June 2022)

Superconductivity has been realized in films of $La_{1-x}Sr_xNiO_2$. Here we report synthesis and characterization of polycrystalline samples of $La_{1-x}Sr_xNiO_3$ and $La_{1-x}Sr_xNiO_2$ ($0 \le x \le 0.2$). Magnetization and resistivity measurements reveal that $La_{1-x}Sr_xNiO_3$ are paramagnetic metal and $La_{1-x}Sr_xNiO_2$ exhibit an insulating behavior. Superconductivity is not detected in bulk samples of $La_{1-x}Sr_xNiO_2$. The absence of superconductivity in bulk $La_{1-x}Sr_xNiO_2$ may be due to the generation of hydroxide during reduction, a small amount of nickel impurity, or incomplete reduction of apical oxygen. The effect of interface in films of $La_{1-x}Sr_xNiO_2$ may also play a role for superconductivity.

Keywords: nickel oxide, superconductivity

PACS: 74.70.–b, 74.25.fc, 74.62.Dh **DOI:** 10.1088/1674-1056/ac7a1a

The discovery of superconductivity in film samples of $Nd_{0.8}Sr_{0.2}NiO_2$ has drawn much attention on nickel oxide materials.[1] In fact, $LaNiO_3$ was studied in 1983 before the discovery of superconductivity in copper oxide materials. $La_{2-x}Sr_xNiO_4$ were investigated because of the structural similarity to the high temperature superconducting (SC) cuprate perovskites $La_{2-x}Sr_xCuO_4$. Superconductivity has also been predicted in nickelate heterostructures like $LaNiO_3$/$LaMO_3$ (M is a trivalent cation, like Al or Ga) superlattices,[2,3] while unconventional superconductivity has not been realized in nickel oxide materials with the oxidation states of Ni^{3+} and Ni^{2+}.[4–6] It was suggested that superconductivity may exist in low spin oxidation state of Ni^{1+} with a square coordination with O^{2-} ions.[7–9] However, the low valent state of nickel is difficult to stabilize through conventional high-temperature-solid state reaction synthesis method.[10,11]

Tuning the valent states of Ni ions in nickelate thin film heterostructures by combining CaH_2 reductant and carrier doping greatly stimulated scientists to explore superconductivity and other novel physical properties in nickel-based oxides.[1,12–21] Infinite layer $RNiO_2$ (R = Nd, La, and Pr) is isostructural to $CaCuO_2$ with two-dimensional NiO_2 planes stacking as NiO_2–R–NiO_2–R layers as shown in Fig. 1. $CaCuO_2$ is one of the parent compounds of high-temperature superconductors. Through hole-doping the antiferromagnetic (AF) order can be suppressed and superconductivity emerges in $(Ca_{1-x}Sr_x)_{1-y}CuO_{2-\delta}$ with the maximum SC transition temperature of $T_c = 110$ K.[22,23] Furthermore, the spin configuration of $Ni^{1+}3d^9$ is similar to that of Cu^{2+} in cuprates. SC domes were observed in films of $R_{1-x}Sr_xNiO_2$ (R = La, Nd, and Pr),[13–15,24] $La_{1-x}Ca_xNiO_2$[25] and $Nd_6Ni_5O_{12}$.[17] AF spin fluctuations were revealed and unconventional mechanism of superconductivity was proposed.[16,26–28] While the superconductivity observed in nickel-based oxides is all in the form of thin film samples,[1,13–15,17,24,29–32] it is worthwhile to explore superconductivity in bulk samples. Recently bulk samples $R_{1-x}Sr_xNiO_2$ (R = Sm, Nd)[33–35] and $La_{1-x}Ca_xNiO_2$[36] were synthesized whereas superconductivity was not detected. So far, electrical and magnetic properties of Sr doped bulk samples of $La_{1-x}Sr_xNiO_2$ have not been reported, where superconductivity has been observed in film samples.

In this paper, we report synthesis and systematic studies of the bulk samples of $La_{1-x}Sr_xNiO_3$ and $La_{1-x}Sr_xNiO_2$ with normal compositions of $0 \le x \le 0.4$. The actual doping level is around $0 \le x \le 0.2$ determined from inductively coupled plasma measurements. $La_{1-x}Sr_xNiO_3$ are synthesized using molten KOH as flux. $La_{1-x}Sr_xNiO_2$ are obtained via a topochemical reduction process from $La_{1-x}Sr_xNiO_3$ using CaH_2 as a reducing agent. Measurements of resistivity, magnetization, and heat capacity are carried out to explore the magnetic and electrical properties. Results of electronic transport show that $La_{1-x}Sr_xNiO_3$ ($0 \le x \le 0.2$) are good metals, while $La_{1-x}Sr_xNiO_2$ exhibit insulating behavior and no superconductivity is observed.

$La_{1-x}Sr_xNiO_3$ with nominal $0 \le x \le 0.4$ were synthesized using KOH as the flux.[37] La_2O_3 was preheated at 1100 °C for one day to remove water then weighed in a glove box filled with argon. Stoichiometric ratios of powders of NiO (99.99%), La_2O_3 (99.9%), and $SrCO_3$ (99.99%) were mixed and heated at 1200 °C for one day. The flux of KOH was heated at 450 °C for 12 h to form O_2^- via the reaction of $3O_2 + 4OH^- \Longleftrightarrow 4O_2^- + 2H_2O$,[38] followed by the mixture of the nickelate oxide powders and dwelled at 450 °C for 10 h. KOH was removed from powders of $La_{1-x}Sr_xNiO_3$ by deion-

†Corresponding author. E-mail: wangmeng5@mail.sysu.edu.cn

izing water. Thereafter the powders were dried at 120 °C. Finally, dark powders of $La_{1-x}Sr_xNiO_3$ were obtained. The topotactic reduction process was demonstrated in Fig. 1. The process was as follows: $La_{1-x}Sr_xNiO_3$ were placed in a crucible and CaH_2 was wrapped with an aluminum foil. They were sealed in an evacuated silica tube at a molar ratio of 1:4. $La_{1-x}Sr_xNiO_2$ were obtained after heating the mixture at 350 °C for 12 h.

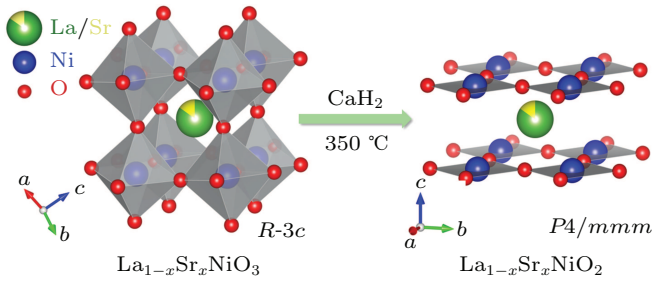

Fig. 1. Structures of $La_{1-x}Sr_xNiO_3$ (left) and $La_{1-x}Sr_xNiO_2$ (right). Upon low temperature reduction with CaH_2 as a reducing agent, the powder samples undergo a topotactic transition from the perovskite phase to the infinite-layer phase.

Crystal structures of the samples were investigated by x-ray diffraction (XRD, Empyrean) at 300 K. The diffraction data were refined by the Rietveld method.[39] The cation contents in powder samples of $La_{1-x}Sr_xNiO_3$ and $La_{1-x}Sr_xNiO_2$ were measured by the inductively coupled plasma (ICP, Atomic Emission Spectrometry, Optima8300). An iodometric titration method was performed to evaluate the content of oxygen in $La_{1-x}Sr_xNiO_3$.[40] The powder samples were dissolved in HCl with KI (0.1 mol/L) solution. The Ni^{3+} ions will be reduced to Ni^{2+} and iodine is generated during the process. The content of iodine could be determined by $Na_2S_2O_3$ (0.01 mol/L) using starch solution as an indicator. Magnetization and resistivity in the temperature range of 3–300 K and heat capacity measurements in the range of 3–200 K were conducted on a physical property measurement system (PPMS, Quantum Design). The electrical resistivity was measured on a pressed bar sample using a standard 4-prob technique.

The crystal structures of $La_{1-x}Sr_xNiO_3$ and $La_{1-x}Sr_xNiO_2$ are shown in Fig. 1. XRD patterns of the two compounds are depicted in Figs. 2(a) and 2(b), respectively. The XRD patterns of $LaNiO_3$ can be indexed as a rhombohedral unit cell and $LaNiO_2$ as a tetragonal unit cell as reported previously.[41–44] The XRD patterns for Sr doped compounds indicate that the powder samples are a single phase for $La_{1-x}Sr_xNiO_3$ with $0 \le x \le 0.15$ and $La_{1-x}Sr_xNiO_2$ with $0.05 \le x \le 0.4$. To simplify the description, the nominal x is used to present samples with distinct compositions in the article. NiO is identified in $La_{1-x}Sr_xNiO_3$ for $x = 0.2$, 0.3, and 0.4. Reflection peaks associated with La_2O_3 can be observed in the XRD pattern of $LaNiO_2$, as shown in Fig. 2. Ni impurity can be observed in $La_{1-x}Sr_xNiO_2$ with $x = 0.3$. Variation of the lattice parameters as a function of the Sr contents is not obvious because the sizes of La^{3+} and Sr^{2+} are similar.[35,45] The refined structural parameters are shown in Table 1.

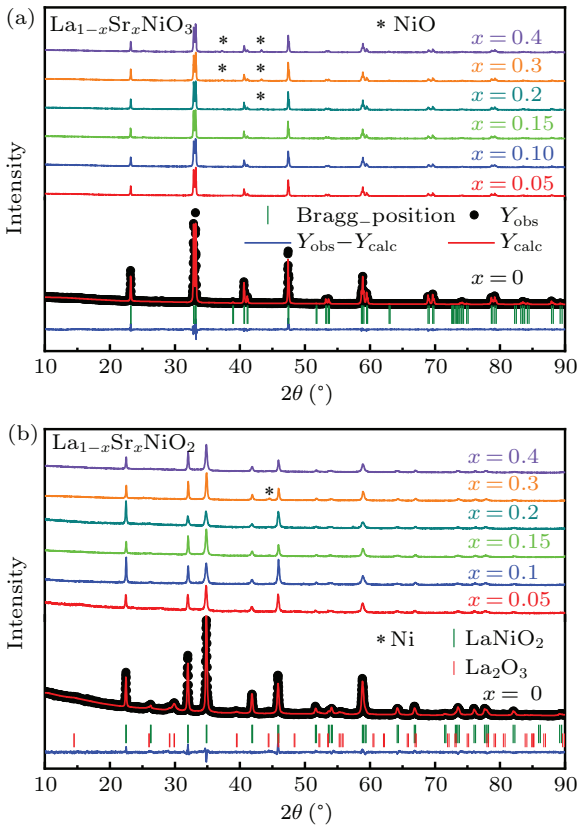

Fig. 2. Ambient powder XRD patterns of (a) $La_{1-x}Sr_xNiO_3$ and (b) $La_{1-x}Sr_xNiO_2$ with nominal compositions of $0 \le x \le 0.4$ with corresponding Rietveld fitting results by using the *R*-3*c* space group and *P*4/*mmm*, respectively. The black dots represent the observed data, the red lines represent the fitting curves, and the blue lines illustrate the differences between the data and fitting. The olive short vertical lines mark the Bragg positions. For comparison the data are shifted vertically. The positions of reflections related to NiO, La_2O_3, and Ni are indicated.

Table 1. Refined structural parameters for $LaNiO_3$ and $LaNiO_2$ at 300 K.

Compound	$LaNiO_3$	$LaNiO_2$
Space group	*R*-3*c*	*P*4/*mmm*
Unit-cell parameters	$a = b = 5.4443(1)$ Å,	$a = b = 3.9559(2)$ Å,
	$c = 13.1569(3)$ Å	$c = 3.3901(2)$ Å
	$\alpha = \beta = 90°$, $\gamma = 120°$	$\alpha = \beta = \gamma = 90°$
Atomic parameters	La (0, 0, 0.25)	La (0.5, 0.5 0.5)
	Ni (0, 0, 0)	Ni (0, 0, 0)
	O (0.45, 0, 0)	O (0, 0.5, 0)
Rietveld *R*-factors	R_p: 0.19	R_p: 0.23
	R_{wp}: 0.14	R_{wp}: 0.16
	R_{exp}: 0.06	R_{exp}: 0.10
Goodness-of-fit on F^2	5.92	2.55

To check the real compositions of the as grown and oxygen removed compounds, we show the actual x verse the nominal x in Fig. 3(a). The relations of the actual and nominal contents of Sr follow the same trend, revealing half of the Sr is successfully doped to the samples. For the nominal $x = 0.4$ compounds, the actual values are $x = 0.21$ and 0.19 for $La_{1-x}Sr_xNiO_3$ and $La_{1-x}Sr_xNiO_2$, respectively. The big error of the actual x in $La_{0.85}Sr_{0.15}NiO_3$ may be due to inhomogeneity of the two samples we measured. The contents of

oxygen are further investigated through the iodometric titration method. In this way, the oxygen content is determined from the ratio of Ni^{3+} and Ni^{2+}. The results as shown in Fig. 3(b) suggest the existence of 12% oxygen vacancies.

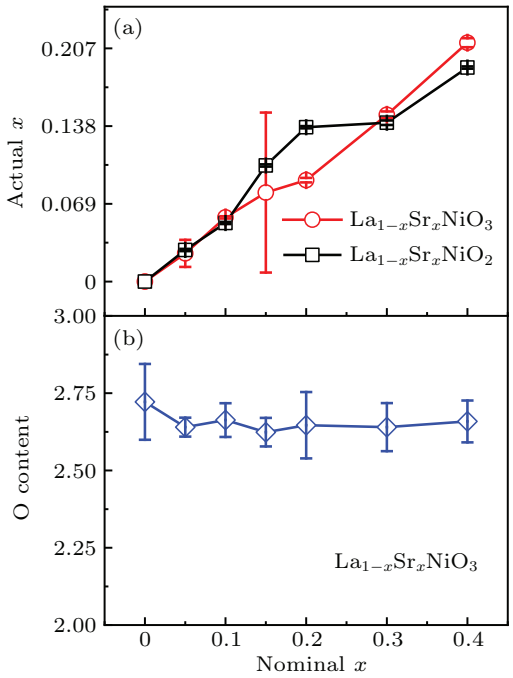

Fig. 3. (a) ICP determined actual x in $La_{1-x}Sr_xNiO_3$ and $La_{1-x}Sr_xNiO_2$. (b) Actual oxygen content of $La_{1-x}Sr_xNiO_3$ measured via the iodometric titration method. The error bars are the standard deviation of the measured results.

Figure 4 displays the temperature dependence of the physical properties of $La_{1-x}Sr_xNiO_3$. The resistivity and magnetization of $LaNiO_3$ are consistent with previous reports that reveal $LaNiO_3$ exhibiting a metallic paramagnetic state with large electronic correlations,[46,47] as shown in Figs. 4(a) and 4(b). The upturn in resistivity below 50 K has been observed in bulk $LaNiO_{3-\delta}$ and suggested to result from defection of oxygen during the synthesis process.[48,49] Upon Sr doping, the metallic behavior of $La_{1-x}Sr_xNiO_3$ is remained, while the magnitude of resistivity changes.

Weak kinks can be identified on magnetization at ~ 22 K in doped compounds. The kink is obvious for $La_{0.8}Sr_{0.2}NiO_3$ measured with $\mu_0 H = 0.1$ T and zero-field cooled (ZFC) mode as shown in Fig. 4(b). The temperatures of the kinks for different compounds locate at the same temperature. To ascertain the origin of the kinks, we carried out measurements of magnetization and specific heat as a function of temperature at various magnetic fields for $La_{0.8}Sr_{0.2}NiO_3$. The magnetization is gradually suppressed as the magnetic field increases, while the temperature of the anomaly is barely changed [Fig. 4(c)]. We repeated the process of synthesis and measurements. The kinks in magnetization for the doped samples are repeatable. However, an anomaly around 22 K is not observed on specific heat at 0 T and 5 T magnetic fields as shown in Fig. 4(d). The kinks are absent in $Nd_{1-x}Sr_xNiO_3$[50] and $Sm_{1-x}Sr_xNiO_3$.[33] It is possible that the abnormal magnetization in $La_{1-x}Sr_xNiO_3$ at 22 K origins from impurities during the synthesis process.

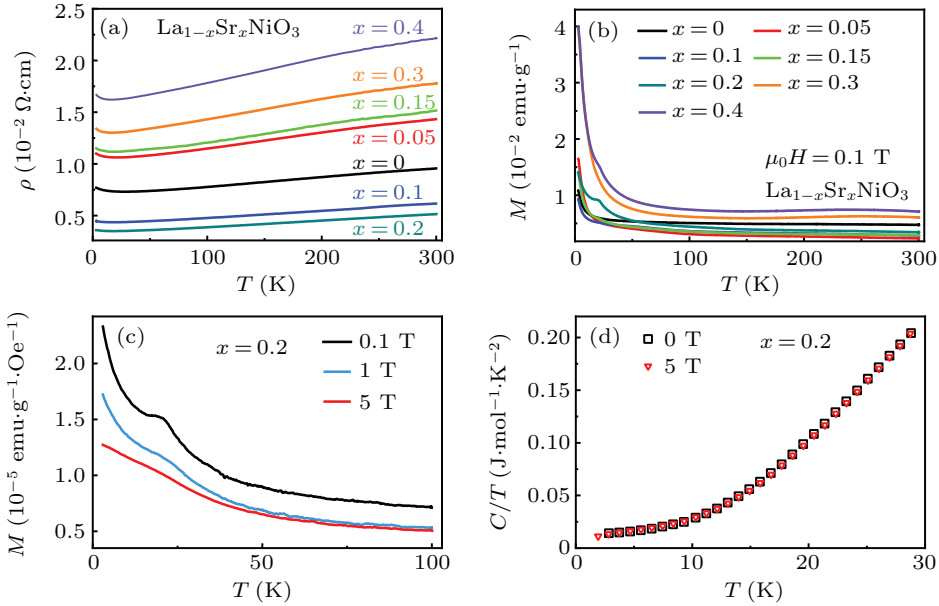

Fig. 4. (a) Resistivity versus temperature $\rho(T)$ plots of $La_{1-x}Sr_xNiO_3$ with nominal compositions of $0 \le x \le 0.4$. (b) Magnetic susceptibility of $La_{1-x}Sr_xNiO_3$ with a field of $\mu_0 H = 0.1$ T. (c) Magnetization for $La_{0.8}Sr_{0.2}NiO_3$ in ZFC process for magnetic fields of $\mu_0 H = 0$ T, 1 T, and 5 T. (d) Specific heat of $La_{0.8}Sr_{0.2}NiO_3$ for 3 K $\le T \le$ 30 K, and $\mu_0 H = 0$ T and 5 T.

To explore the possible superconductivity in the bulk samples of $La_{1-x}Sr_xNiO_2$, we performed resistivity and magnetization measurements of $La_{1-x}Sr_xNiO_2$ as shown in Fig. 5. The resistivity versus temperature $\rho(T)$ of $La_{1-x}Sr_xNiO_2$ in zero applied magnetic field in Fig. 4(a) reveals semiconducting-like behavior. The doped Sr does not affect the electronic properties severally. No superconductivity is observed in the bulk samples. In Fig. 5(b), we

show the fittings by using the activation-energy model $\rho(T) = \rho_0 \exp(E/k_B T)$ through fitting the high temperature resistivity data from 200 K to 300 K, where ρ_0 is a prefactor and k_B is the Boltzmann constant.[34,51–53] The resultant thermal activation energies are between 35–55 meV, as shown in the inset of Fig. 5(b). To explore the magnetic properties of $La_{1-x}Sr_xNiO_2$, we show magnetization and magnetoresistance as functions of magnetic field and temperature in Figs. 5(c) and 5(d). The magnetization measured in field cooling (FC) deviates from that of ZFC in a wide temperature range, indicating a spin glass state. Figure 5(d) displays temperature dependence of the magnetoresistance (MR) of $LaNiO_2$. The MR effect changes sign from negative at 3 K, 10 K, and 20 K to positive at 30 K and 50 K, similar to the observation in films of $Nd_{0.8}Sr_{0.2}NiO_2$.[34] The sign reversal of the MR upon changing temperature suggests the existence of magnetic order or magnetic correlations. Figure 5(e) shows a typical hysteresis of ferromagnetism (FM) vs. magnetic field at various temperatures measured at $T = 3$ K, 50 K, 300 K, and 650 K. The FM is reminiscent of the resident nickel in Sr doped $RNiO_2$.[33,34,54] Therefore, magnetic susceptibility is measured from 300 K to 1000 K to verify the existence of Ni. As shown in Fig. 5(f), the ferromagnetic transition of Ni at $T_c = 627$ K is identified in bulk $LaNiO_2$. However, XRD measurements on powder samples of $LaNiO_2$ did not reveal the existence of Ni, indicating a low content of Ni impurity in the samples. Thus, the spin-glass like behavior may be due to the Ni impurity. Small amount of Ni in the sample would not change the electronic transport properties. The MR effect should be the intrinsic properties of $LaNiO_2$ and induced by magnetic correlations that have been proposed by Raman scattering measurements on $NdNiO_2$[55] and x-ray magnetic linear dichroism measurements on $Nd_{0.8}Sr_{0.8}NiO_2$ films.[27]

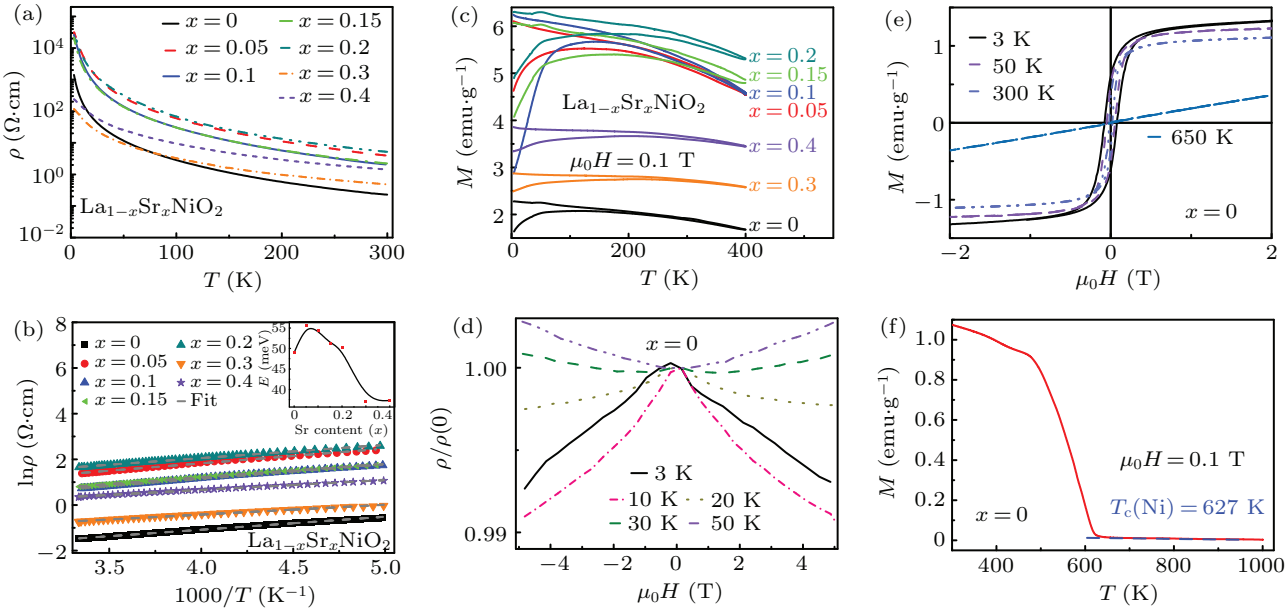

Fig. 5. (a) Resistivity of $La_{1-x}Sr_xNiO_2$ as a function of temperature from 3 K to 300 K and (b) fits using the activation-energy model $\rho(T) = \rho_0 \exp(E/k_B T)$ from 200 K to 300 K. The inset shows the thermal activation energies against the Sr content. (c) Magnetic susceptibility measured under ZFC and FC conditions for 3 K $\leq T \leq$ 400 K and $\mu_0 H = 0.1$ T. (d) Magnetoresistance for $LaNiO_2$ at $T = 3$ K, 10 K, 20 K, 30 K, and 50 K. (e) Magnetization of $LaNiO_2$ at $T = 3$ K, 50 K, 300 K, and 650 K. (f) Magnetic susceptibility of $LaNiO_2$ from 300 K to 1000 K with $\mu_0 H = 0.1$ T.

As theoretical calculations, $RNiO_2$ are metal.[12,56–58] However, resistivity measurements reveal that bulk samples of $RNiO_2$ are semiconductors. It has been suggested that the difference between theoretical predictions and experimental observations could be ascribed to hydrogens that take place the apical oxygen sites to reduce the thermodynamical instability.[59] Small size of hydrogen can insert into the samples and form oxide hydride $La_{1-x}Sr_xNiO_yH_z$ which exhibit insulating behavior. This has been observed in $NdNiO_xH_y$ ($x \sim 2.3$, $y \sim 0.7$),[60] $BaTiO_{3-x}H_x$,[61] $Sr_3Co_2O_{4.33}H_{0.84}$,[62] and $LaSrCoO_3H_{0.7}$.[63] In addition, impurity and incomplete reduction of the apical oxygens in $RNiO_2$ could also result in large resistivity.[43,64] It is known that the purity of films is essential for realizing superconductivity in $Nd_{1-x}Sr_xNiO_2$ films.[29,30] The absence of superconductivity in bulk samples may be due to the deviation of O^{2-} ions amount and the existence of Ni impurity. The interfaces between the substrate of $SrTiO_3$ and $La_{1-x}Sr_xNiO_2$ films may play a role in the magnetic correlations and emergence of superconductivity.[42,65–67] Further studies on high quality single crystals of $La_{1-x}Sr_xNiO_2$ are required.

In conclusion, we synthesized polycrystalline samples $La_{1-x}Sr_xNiO_3$ and $La_{1-x}Sr_xNiO_2$ with an actual doping level of $0 \leq x \leq 0.2$ and characterized their properties. The samples of $La_{1-x}Sr_xNiO_3$ are prepared using KOH as the flux. $La_{1-x}Sr_xNiO_2$ are synthesized by removing the api-

cal oxygen from $La_{1-x}Sr_xNiO_3$ using CaH_2 as a reducing agent. $La_{1-x}Sr_xNiO_3$ are good metals as expectation. While $La_{1-x}Sr_xNiO_2$ exhibit insulating behavior, differing from theoretical calculations. No evidence of superconductivity is observed. The Ni impurity, resident apical oxygens, inserted hydrogens in bulk $La_{1-x}Sr_xNiO_2$ may mask the fundamental magnetic properties and inhibit the achievement of superconductivity.

Acknowledgements

Work at Sun Yat-Sen University was supported by the National Natural Science Foundation of China (Grant Nos. 12174454, 11904414, 11904416, and U2130101), the Guangdong Basic and Applied Basic Research Foundation (Grant No. 2021B1515120015), the Guangzhou Basic and Applied Basic Research Foundation (Grant No. 202201011123), and the National Key Research and Development Program of China (Grant No. 2019YFA0705702).

References

[1] Li D, Lee K, Wang B Y, *et al*. 2019 *Nature* **572** 624
[2] Chaloupka J and Khaliullin G 2008 *Phys. Rev. Lett.* **100** 016404
[3] Hansmann P, Yang X, Toschi A, *et al*. 2009 *Phys. Rev. Lett.* **103** 016401
[4] Zhou G, Jiang F, Zang J, *et al*. 2018 *ACS Appl. Mater.* **10** 1463
[5] Klimczuk T, McQueen T M, Williams A J, *et al*. 2009 *Phys. Rev. B* **79** 012505
[6] Liu H, Hu X, Guo H, *et al.* 2022 arXiv:2205.00116
[7] Anisimov V I, Bukhvalov D and Rice T M 1999 *Phys. Rev. B* **59** 7901
[8] Botana A S, Pardo V and Norman M R 2017 *Phys. Rev. Mater.* **1** 021801
[9] Zhang J, Botana A S, Freeland J W, *et al*. 2017 *Nat. Phys.* **13** 864
[10] Li Q, He C, Zhu X, *et al*. 2020 *Sci. Chin. Phys. Mech. Astron.* **64** 227411
[11] Liu Z, Sun H, Huo M, *et al*. 2022 arXiv:2205.00950
[12] Gu Y, Zhu S, Wang X, *et al*. 2020 *Commun. Phys.* **3** 84
[13] Osada M, Wang B Y, Goodge B H, *et al*. 2020 *Nano Lett.* **20** 5735
[14] Osada M, Wang B Y, Lee K, *et al*. 2020 *Phys. Rev. Mater.* **4** 121801
[15] Zeng S, Tang C S, Yin X, *et al*. 2020 *Phys. Rev. Lett.* **125** 147003
[16] Lu H, Rossi M, Nag A, *et al*. 2021 *Science* **373** 213
[17] Pan G A, Ferenc Segedin D, LaBollita H, *et al*. 2022 *Nat. Mater.* **21** 160
[18] Gao J, Peng S, Wang Z, *et al.* 2021 *Natl. Sci. Rev.* **8** nwaa218
[19] Hao J, Fan X, Li Q, *et al*. 2021 *Phys. Rev. B* **103** 205120
[20] Gu Q, Li Y, Wan S, *et al*. 2020 *Nat. Commun.* **11** 6027
[21] Gu Q and Wen H H 2022 *Innovation (N Y)* **3** 100202
[22] Azuma M, Hiroi Z, Takano M, *et al*. 1992 *Nature* **356** 775
[23] Hiroi Z, Azuma M, Takano M, *et al*. 1993 *Physica C* **208** 286
[24] Osada M, Wang B Y, Goodge B H, *et al.* 2021 *Adv. Mater.* **33** 2104083
[25] Zeng S, Li C, Chow L E, *et al.* 2022 *Sci. Adv.* **8** eabl9927
[26] Cui Y, Li C, Li Q, *et al*. 2021 *Chin. Phys. Lett.* **38** 067401
[27] Zhou X, Zhang X, Yi J, *et al.* 2022 *Adv. Mater.* **34** 2106117
[28] Zhou T, Gao Y and Wang Z 2020 *Sci. Chin. Phys. Mech. Astron.* **63** 287412
[29] Gao Q, Zhao Y, Zhou X J, *et al*. 2021 *Chin. Phys. Lett.* **38** 077401
[30] Lee K, Goodge B H, Li D, *et al*. 2020 *APL Mater.* **8** 041107
[31] Xiang Y, Li Y, Li Y, *et al*. 2021 *Chin. Phys. Lett.* **38** 047401
[32] Ding X, Shen S, Leng H, *et al*. 2022 *Sci. Chin. Phys. Mech. Astron.* **65** 267411
[33] He C, Ming X, Li Q, *et al*. 2021 *J. Phys. Condens Matter.* **33** 265701
[34] Li Q, He C, Si J, *et al*. 2020 *Commun. Mater.* **1** 16
[35] Wang B X, Zheng H, Krivyakina E, *et al*. 2020 *Phys. Rev. Mater.* **4** 084409
[36] Puphal P, Wu Y M, Fursich K, *et al*. 2021 *Sci. Adv.* **7** eabl8091
[37] Shivakumara C, Hegde M S, Prakash A S, *et al*. 2003 *Solid State Sci.* **5** 351
[38] Mugavero S J, Gemmill W R, Roof I P, *et al*. 2009 *J. Solid State Chem.* **182** 1950
[39] Rietveld H M 1969 *J. Appl. Crystallogr.* **2** 65
[40] Licci F, Turilli G and Ferro P 1997 *J. Magn. Magn. Mater.* **170** 240
[41] Kawai M, Inoue S, Mizumaki M, *et al*. 2009 *Appl. Phys. Lett.* **94** 082102
[42] Geisler B and Pentcheva R 2021 *Phys. Rev. Research* **3** 013261
[43] Hayward M A, Green M A, Rosseinsky M J, *et al*. 1999 *J. Am. Chem. Soc.* **121** 8843
[44] Rodríguez E, Álvarez I, López M L, *et al*. 1999 *J. Solid State Chem.* **148** 479
[45] Alonso J A, Martínez-Lope M J and Hidalgo M A 1995 *J. Solid State Chem.* **116** 146
[46] Guo H, Li Z W, Zhao L, *et al*. 2018 *Nat. Commun.* **9** 43
[47] Zhou J S, Marshall L G and Goodenough J B 2014 *Phys. Rev. B* **89** 245138
[48] Gayathri N, Raychaudhuri A K, Xu X Q, *et al*. 1998 *J. Phys. Condens. Matter* **11** 2901
[49] Rajeev A T A K P 1999 *J. Phys. Condens. Matter* **11** 3291
[50] Yang H, Wen Z, Shu J, *et al*. 2021 *Solid State Commun.* **336** 114420
[51] Yin J, Wu C, Li L, *et al*. 2020 *Phys. Rev. Mater.* **4** 013405
[52] Sun H, Chen C, Hou Y, *et al*. 2021 *Sci. Chin. Phys. Mech. Astron.* **64** 118211
[53] Li L, Hu X, Liu Z, *et al*. 2021 *Sci. Chin. Phys. Mech. Astron.* **64** 287412
[54] Crespin M, Isnard O, Dubois F, *et al*. 2005 *J. Solid State Chem.* **178** 1326
[55] Fu Y, Wang L, Cheng H, *et al*. 2020 arXiv:1911.03177
[56] Liu Z, Z. Ren, W. Zhu, *et al*. 2020 *npj Quantum Mater.* **5** 31)
[57] Islam M, Koley S and Basu S 2021 *Eur. Phys. J. B* **94** 187
[58] Krishna J, LaBollita H, Fumega A O, *et al*. 2020 *Phys. Rev. B* **102** 224506
[59] Si L, Xiao W, Kaufmann J, *et al*. 2020 *Phys. Rev. Lett.* **124** 166402
[60] Onozuka T, Chikamatsu A, Katayama T, *et al*. 2016 *Dalton Trans.* **45** 12114
[61] Kobayashi Y, Hernandez O J, Sakaguchi T, *et al*. 2012 *Nat. Mater.* **11** 507
[62] Helps R M, Rees N H and Hayward M A 2010 *Inorg. Chem.* **49** 11062
[63] Hayward M A, Cussen E J, Claridge J B, *et al*. 2002 *Science* **295** 1882
[64] Zhou X R, Feng Z X, Qin P X, *et al*. 2020 *Rare Metals* **39** 368
[65] Bernardini F and Cano A 2020 *J. Phys. Matter* **3** 03
[66] He R, Jiang P, Lu Y, *et al*. 2020 *Phys. Rev. B* **102** 035118
[67] Ortiz R A, Menke H, Misják F, *et al*. 2021 *Phys. Rev. B* **104** 165137